Progress of Theoretical Physics, Vol. 100, No. 4, October 1998

Quark and Lepton Mass Matrix in an Asymptotically Non-Free Theory

Masako BANDO, Joe SATO* and Koichi YOSHIOKA**

Aichi University, Miyoshi-cho, Aichi 470-02, Japan
**Department of Physics, University of Tokyo, Tokyo 133-0033, Japan*
***Department of Physics, Kyoto University, Kyoto 606-8502, Japan*

(Received June 17, 1998)

We analyze fermion mass-matrix structure in an asymptotically non-free model with $4+\bar{1}$ generations. The texture at the GUT scale is uniquely determined by supposing that the masses of heavy up-type quarks (charm as well as top) are realized as their infrared fixed point values. By assuming $SO(10)$ GUT-like relations for Yukawa couplings in this model, this texture can explain all fermion masses and quark mixing with only one small parameter, which is almost equal to the Cabibbo angle.

§1. Introduction

Determining the origin of fermion masses and mixing is one of the most important problems in constructing matter unification models. In the framework of the minimal supersymmetric standard model (MSSM), which is successful in attaining gauge coupling unification,[1] there are many works dedicated to obtaining fermion mass structure.[2] One interesting feature which has been found is that the MSSM with the $SU(5)$-GUT relation is almost consistent with the observed bottom-tau mass ratio.[3]

In previous papers,[4),5] we investigated an extension of the MSSM with an asymptotically non-free (ANF) property motivated by the possibility of dynamical gauge bosons. The difference between dynamical gauge bosons and elementary gauge bosons is the existence of the compositeness condition at some scale below which they behave as if they are asymptotically non-free gauge fields.[6] It is interesting to determine whether or not the present standard gauge theory with ANF character preserves the above good predictions of the MSSM. As an example we consider the simplest case in which there are 2 extra generations, forming a generation-mirror generation pair (the 4th and anti-4th generations) with $SU(2)_W \times U(1)_Y$ invariant Dirac masses M. There are many works that address the idea of extra fermions, especially vector-like families, which are motivated by various physical backgrounds, string models,[7] composite models,[8] grand unified models,[9] etc., and the possibility of having new families just above the 3-generation families is interesting. This vector-like matter is compatible with the constraints determined by the LEP measurements, namely the so-called Peskin-Takeuchi constraints.[10] Following Babu and Pati in Ref. 9), we call this the extended supersymmetric standard model (ESSM) hereafter. In the ESSM three gauge couplings are also unified at almost the same scale as that of the MSSM but with different unified coupling. An immediate consequence of the ESSM is that

all three gauge couplings of $SU(3)_C, SU(2)_W$ and $U(1)_Y$, are ANF: they become larger as they evolve up to coincide at the unification scale. This model is a typical one in which the asymptotically non-free gauge couplings remain reasonably small up to the GUT scale (see Ref. 4) and references therein), and the model is worth investigating.

Another interesting feature of the ESSM is the infrared fixed-point structure of Yukawa couplings due to the ANF gauge couplings. In Ref. 5), we pointed out that the top and bottom quark masses are reproduced as infrared fixed point (IRFP) predictions, which are almost insensitive to initial GUT conditions due to the ANF characters of gauge couplings. Such strong convergence of Yukawa couplings to their infrared fixed points is a common feature appearing in ANF theories.[12] In such a case, the IRFP structure acts to translate symmetry structures into quantitative predictions for low-energy physical parameters, as stressed in Ref. 13). We demonstrated how strongly the couplings are focused into their infrared fixed points in ANF theories as well as the structure of the renormalization-group flows by comparing the ESSM with the MSSM.[5]

In the above-mentioned analyses, we neglected the small Yukawa couplings of the first and second generations. However, the existence of Yukawa couplings to the 4th and $\bar{4}$th generations may affect their structure in some way. In this paper we study the fermion masses of 5 full generations. As is well known, the ordinary fermion masses show typical hierarchical structures with small parameters $\sim O(10^{-(1\text{-}3)})$, which have to be introduced from the beginning in GUT textures. In the ESSM case we have one more hierarchical factor; the ratio of the usual $SU(2)_W \times U(1)_Y$ breaking mass m and the invariant mass M ($m \ll M$). By making full use of the infrared fixed point structure and the hierarchical ratio m/M, we shall determine their textures at the GUT scale.

In §2 we give a quick summary of the present status of the fermion masses and mixing and of some features of our previous analysis in the ESSM. In §3 we analyse the simplest case in which the invariant mass appears only in the 4th and $\bar{4}$th fermions. It is found that the texture at the GUT scale is uniquely determined if we impose the condition that the masses of heavy up-type quarks are realized as their infrared fixed point values, together with $SO(10)$ GUT-like relations for Yukawa couplings. We will see that this texture reproduces the fermion masses and quark mixing by introducing only one small parameter $\epsilon \sim 0.2$, which is almost equal to the Cabibbo angle. Concluding remarks and comments are made in §4. Appendix A is devoted to more complicated analysis in which more invariant masses M are included or texture is non-symmetric. We find that none of them can reproduce the present experimental data of masses and mixing. The renormalization group equations in the ESSM are given in Appendix B.

§2. Fermion masses and mixing

2.1. *Issues of fermion mass*

The possible sources which determine fermion masses are as follows.

1. The texture of Yukawa matrix at the GUT scale:[14] The GUT relations of Yukawa couplings are important to account for the hierarchical structure between generations. Although no rational basis is known to determine the intergenerational relationship, fermion masses seem to exhibit typical hierarchical structures. This may indicate the existence of a kind of generation quantum numbers. Actually there are many papers to explain hierarchical Yukawa couplings by assuming horizontal symmetry,[15] using anomalous $U(1)$,[16] etc., where we can make an active use of higher dimensional operators which effectively give very small Yukawa couplings. In any case it is important to determine the texture of the Yukawa matrix at the GUT scale according to some yet unknown rule. We shall determine the texture phenomenologically assuming that some unknown mechanism yields hierarchical structure.
2. Running couplings from the GUT scale to weak scale: Once we fix the texture at GUT scale the renormalization group equations (RGE) tell us the resultant Yukawa couplings at low-energy scale. Since the Yukawa couplings, except for those of third generation, are much smaller than the strength of gauge couplings (especially the QCD coupling), usually the renormalization effect comes mainly from QCD. The relative ratio between quark Yukawa couplings is not largely changed by RGE. The only important factor is the ratio of Yukawa couplings of quarks and leptons.
3. Mixing pattern of light Higgses: For the moment we treat the Higgs potential, and Higgs mixing (including $\tan\beta$), as free parameters to be determined phenomenologically, since we always encounter the well-known fine-tuning problem.

For later convenience, we list the masses of the present existing fermions at M_Z scale:[17]

$$\begin{array}{lll} m_u \sim 2.33^{+0.42}_{-0.45}\ \text{MeV}, & m_d \sim 4.69^{+0.60}_{-0.66}\ \text{MeV}, & m_e \sim 0.486847\ \text{MeV}, \\ m_c \sim 677^{+56}_{-61}\ \text{MeV}, & m_s \sim 93.4^{+11.8}_{-13.0}\ \text{MeV}, & m_\mu \sim 102.75\ \text{MeV}, \\ m_t \sim 181 \pm 13\ \text{GeV}, & m_b \sim 3.00 \pm 0.11\ \text{GeV}, & m_\tau \sim 1.7467\ \text{GeV}. \end{array} \quad (2\cdot1)$$

2.2. *Mixing angles*

The observed values for the CKM matrix elements are[18]

$$|V_{\text{CKM}}| = \begin{pmatrix} 0.9745 - 0.9757 & 0.219 - 0.224 & 0.002 - 0.005 \\ 0.218 - 0.224 & 0.9736 - 0.9750 & 0.036 - 0.046 \\ 0.004 - 0.014 & 0.034 - 0.046 & 0.9989 - 0.9993 \end{pmatrix}. \quad (2\cdot2)$$

These data also indicate hierarchical structure:

$$\theta_{12} \sim \sin\theta_C \equiv \lambda \sim 0.22, \qquad \theta_{23} \sim \lambda^2, \qquad \theta_{13} \equiv x \sim \lambda^{3\text{-}4}. \quad (2\cdot3)$$

It is interesting to note the following relations between the mixing angles and the relevant mass eigenvalues (at M_Z scale):

- $\theta_{12} \sim 0.22$

$$\sqrt{m_u/m_c} = 0.051 \sim 0.067, \qquad \sqrt{m_d/m_s} = 0.196 \sim 0.256, \quad (2\cdot4)$$

- $\theta_{13} \sim 0.003$

$$\sqrt{m_u/m_t} = 0.003 \sim 0.004, \qquad \sqrt{m_d/m_b} = 0.036 \sim 0.043, \tag{2·5}$$

- $\theta_{23} \sim 0.037$

$$\sqrt{m_c/m_t} = 0.056 \sim 0.066, \qquad \sqrt{m_s/m_b} = 0.161 \sim 0.191, \tag{2·6}$$

where the mixing angles may be related to the ratios of the mass eigenvalues by taking the following down [19] and up [20] side mass matrices via the seesaw mechanism:

$$m_D^{(12)} = \begin{array}{c} \\ 1 \\ 2 \end{array} \begin{array}{c} \begin{array}{cc} 1 & 2 \end{array} \\ \begin{pmatrix} 0 & \lambda \\ \lambda & 1 \end{pmatrix} \end{array} \cdot m_s \,, \tag{2·7}$$

and

$$m_U^{(13)} = \begin{array}{c} \\ 1 \\ 3 \end{array} \begin{array}{c} \begin{array}{cc} 1 & 3 \end{array} \\ \begin{pmatrix} 0 & x \\ x & 1 \end{pmatrix} \end{array} \cdot m_t \,. \tag{2·8}$$

However, the 2-3 mixing is too small compared with the mass ratio in either the up or down sector. We need a more complicated mechanism which may be the combination of mixing in both up and down sectors.

2.3. *Fermion masses of third generation in ESSM*

Before proceeding to the analysis of the full fermion masses in the ESSM we make a quick review of our previous results for the third generation fermion masses.

The characteristic features of the ESSM are that, due to the ANF character, the Yukawa couplings approach their infrared fixed points very rapidly and that the RGE effect of QCD on the quark enhances down to charged lepton mass ratio by a factor of approximately 5 – 6. This is much more than in the MSSM case, in which this factor is ~ 3. One might think that this QCD enhancement will make it impossible to bring the low-energy bottom-tau mass ratio $R_{b/\tau}(M_Z)$ down to the experimental value ($1.6 \sim 1.8$) even with large Yukawa couplings (large $\tan\beta$). However, if we adopt the unification condition of an $SO(10)$ GUT with a $\overline{126}$-Higgs, the extra enhancement from QCD is actually welcome, since $R_{b/\tau}$ must be enhanced by a factor of 5 – 6 to reproduce the experimental value of $R_{b/\tau}$,

$$Y_t(M_{\rm GUT}) = Y_b(M_{\rm GUT}) = \frac{1}{3} Y_\tau(M_{\rm GUT}) \;\; \rightarrow \;\; R_{b/\tau}(M_Z) \sim \frac{5 \sim 6}{3}. \tag{2·9}$$

Another remarkable result is that due to the ANF gauge couplings, the top and bottom Yukawa couplings are determined almost independently of their initial values fixed at GUT scale. Indeed these Yukawa couplings reach to their fixed points, which are physically significant and provide us with reliable predictions of low-energy parameters. By using these fixed-point solutions and the experimental

value of $\alpha_3(1\text{ TeV}) \sim 0.093$, we obtain, for example,*)

$$m_t(M_Z) \sim 178\,\text{GeV}, \quad m_b(M_Z) \sim 3.2\,\text{GeV}. \qquad (\tan\beta \sim 58) \tag{2·10}$$

These values are certainly consistent with the experimental values. [18]

§3. Mass texture and IR fixed points

We consider the following extended supersymmetric standard model with 5 generations, the MSSM (3 generations) + 1 extra vector-like family $(4+\bar{4})$. The matter content of this model is

$$Q_i,\ u_i,\ d_i,\ L_i,\ e_i\,, \quad (i=1,\cdots,4) \tag{3·1}$$

$$\bar{Q},\ \bar{u},\ \bar{d},\ \bar{L},\ \bar{e}\,, \quad (i=\bar{4}) \tag{3·2}$$

$$H,\ \bar{H},\ \Phi\,. \tag{3·3}$$

In addition to H and $\bar{H}$, which form a pair of $SU(2)_W$ doublet Higgs fields, we have Φ, a (standard gauge group) singlet Higgs which yields masses of the extra vector-like family. In this paper, we consider one Φ, which attains a vacuum expectation value on the order of the TeV scale, [8)-11)] by taking suitably soft SUSY breaking terms of Φ. In this situation, the superpotential becomes

$$\begin{aligned} W \;=\; & \sum_{i,j=1,\cdots,4} \left(\boldsymbol{Y}_{u_{ij}} \epsilon_{ab} Q_i^a u_j \bar{H}^b + \boldsymbol{Y}_{d_{ij}} \epsilon_{ab} Q_i^a d_j H^b + \boldsymbol{Y}_{e_{ij}} \epsilon_{ab} L_i^a e_j H^b \right) \\ & + Y_{\bar{u}} \bar{Q}_a \bar{u} H^a + Y_{\bar{d}} \bar{Q}_a \bar{d} \bar{H}^a + Y_{\bar{e}} \bar{L}_a \bar{e} \bar{H}^a + Y \Phi^3 \\ & + \sum_{i=1,\cdots,4} \left(Y_{Q_i} \Phi Q_i^a \bar{Q}_a + Y_{u_i} \Phi u_i \bar{u} + Y_{d_i} \Phi d_i \bar{d} + Y_{L_i} \Phi L_i^a \bar{L}_a + Y_{e_i} \Phi e_i \bar{e} \right), \end{aligned} \tag{3·4}$$

where the subscripts i, j and a, b are indices of generation and $SU(2)_W$, respectively, and other indices are trivially contracted. With this superpotential, after $SU(2)_W \times U(1)_Y$ breaking, the forms of the 5×5 fermion mass matrices can be written as

$$m_U = \begin{array}{c} \\ u_{1L} \\ \vdots \\ u_{4L} \\ u_{\bar{4}L} \end{array} \begin{array}{c} \begin{array}{cccc} u_{1R} & \cdots & u_{4R} & u_{\bar{4}R} \end{array} \\ \begin{pmatrix} & \boldsymbol{Y}_{u_{ij}} v_u & & Y_{Q_i} V \\ & & & \\ & Y_{u_i} V & & Y_{\bar{u}} v_d \end{pmatrix} \end{array}, \tag{3·5}$$

$$m_D = \begin{array}{c} \\ d_{1L} \\ \vdots \\ d_{4L} \\ d_{\bar{4}L} \end{array} \begin{array}{c} \begin{array}{cccc} d_{1R} & \cdots & d_{4R} & d_{\bar{4}R} \end{array} \\ \begin{pmatrix} & \boldsymbol{Y}_{d_{ij}} v_d & & Y_{Q_i} V \\ & & & \\ & Y_{d_i} V & & Y_{\bar{d}} v_u \end{pmatrix} \end{array}, \tag{3·6}$$

*) The tau-lepton Yukawa coupling generally has no infrared fixed-point solution since it does not have a strong $SU(3)$ interaction. We then treat it as an input parameter and determine the value of $\tan\beta$ from the experimental value for $m_\tau(M_Z)$.

$$m_E = \begin{array}{c} \\ e_{1L} \\ \vdots \\ e_{4L} \\ e_{\bar{4}L} \end{array} \begin{array}{c} \begin{array}{cccc} e_{1R} & \cdots & e_{4R} & e_{\bar{4}R} \end{array} \\ \begin{pmatrix} & \boldsymbol{Y}_{e_{ij}} v_d & & Y_{L_i} V \\ & & & \\ & Y_{e_i} V & & Y_{\bar{e}} v_u \end{pmatrix} \end{array}, \tag{3·7}$$

$$\langle H \rangle = \begin{pmatrix} v_d \\ 0 \end{pmatrix}, \quad \langle \bar{H} \rangle = \begin{pmatrix} 0 \\ v_u \end{pmatrix}, \quad \langle \Phi \rangle = V, \tag{3·8}$$

where $u_{iL}, d_{iL}, e_{iL}, (u_{\bar{4}R})^C, (d_{\bar{4}R})^C$ and $(e_{\bar{4}R})^C$ are fermionic components of $SU(2)_W$ doublet fields, and $(u_{iR})^C, (d_{iR})^C, (e_{iR})^C, u_{\bar{4}L}, d_{\bar{4}L}$ and $e_{\bar{4}L}$ are those of $SU(2)_W$ singlets.

3.1. *Candidate for texture and IR fixed points*

Before discussing realistic texture, we classify the types of texture which yield hierarchical masses, referring to their infrared behavior. Since we know that the usual quark and lepton mass matrices exhibit generally typical hierarchical structures, we first consider the dominant part of the matrices including only the 3rd, 4th and $\bar{4}$th generations and then include less important contributions step-by-step. Hereafter, for simplicity $m, \bar{m}$ and M are used symbolically to represent $\boldsymbol{Y}_{f_{ij}} v_{u,d}, Y_{\bar{f}} v_{u,d}$ and $Y_{f_i} V$ $(f = u, d, e)$, respectively, since in our classification only the order of their masses are important $(m \ll M)$. For the moment, let us restrict ourselves to the situation in which Yukawa couplings, $\boldsymbol{Y}_{f_{ij}}$, are symmetric (at the GUT scale) and only the 4th generation couples to the $\bar{4}$th generation forming an invariant mass term M. Analyses for general situations are performed in Appendix A.

First let us consider the dominant matrices (for the 3rd, 4th and $\bar{4}$th generations). For $m \ll M$, after diagonalization at low energy, two of the three eigenvalues are on the order of M, and one eigenvalue m_{33} is small compared with M. In order to get non-zero m_{33}, there are three candidates for the textures classified by their determinants:

- case 1

$$\begin{array}{c} \\ 3 \\ 4 \\ \bar{4} \end{array} \begin{array}{c} \begin{array}{ccc} 3 & 4 & \bar{4} \end{array} \\ \begin{pmatrix} m & & 0 \\ & & M \\ 0 & M & \end{pmatrix} \end{array}, \qquad \det{}_{3\times 3} \sim M^2 m, \tag{3·9}$$

$$m_{33} \sim m. \tag{3·10}$$

- case 2

$$\begin{array}{c} \\ 3 \\ 4 \\ \bar{4} \end{array} \begin{array}{c} \begin{array}{ccc} 3 & 4 & \bar{4} \end{array} \\ \begin{pmatrix} 0 & m & 0 \\ m & & M \\ 0 & M & \bar{m} \end{pmatrix} \end{array}, \qquad \det{}_{3\times 3} \sim m^2 \bar{m}, \tag{3·11}$$

$$m_{33} \sim \left(\frac{m\bar{m}}{M^2}\right) m. \tag{3·12}$$

- case 3

$$\begin{array}{c} \\ 3 \\ 4 \\ \bar{4} \end{array} \begin{array}{c} \begin{array}{ccc} 3 & 4 & \bar{4} \end{array} \\ \begin{pmatrix} 0 & m & 0 \\ m & m & M \\ 0 & M & 0 \end{pmatrix} \end{array}, \qquad \det{}_{3\times 3} \sim 0, \tag{3·13}$$

$$m_{33} \sim \text{(radiatively induced)}. \tag{3·14}$$

Here and hereafter, if an element is 0 it is implied that it should be exactly zero at the GUT scale. A blank entry corresponds to the case in which it can be either zero or nonzero. For case 3, the determinant of this texture is zero. However, this type of matrix induces an appreciable non-zero Y_{33} element via the renormalization group, and the resultant low-energy determinant (and eigenvalue m_{33}) cannot be neglected.

Next, we include the second generation and consider 4×4 matrices. In order to obtain hierarchical mass eigenvalues after diagonalization, $m_{22} \ll m_{33} \ll M$, it is needed to realize the hierarchical determinants $\det_{4\times 4}/\det_{3\times 3} \ll m_{33}$. Then the resultant 4×4 textures which realize this hierarchical structure are found to be the following for each case:

- case 1

  There are two distinct types of texture.

  - type A

$$\begin{array}{c} \\ 2 \\ 3 \\ 4 \\ \bar{4} \end{array} \begin{array}{c} \begin{array}{cccc} 2 & 3 & 4 & \bar{4} \end{array} \\ \begin{pmatrix} 0 & 0 & m & 0 \\ 0 & m & & 0 \\ m & & & M \\ 0 & 0 & M & \bar{m} \end{pmatrix} \end{array}, \qquad \det{}_{4\times 4} \sim m^3\bar{m}, \tag{3·15}$$

$$m_{22} \sim \left(\frac{m\bar{m}}{M^2}\right) m. \tag{3·16}$$

  - type B

$$\begin{array}{c} \\ 2 \\ 3 \\ 4 \\ \bar{4} \end{array} \begin{array}{c} \begin{array}{cccc} 2 & 3 & 4 & \bar{4} \end{array} \\ \begin{pmatrix} 0 & 0 & m & 0 \\ 0 & m & & 0 \\ m & & m & M \\ 0 & 0 & M & 0 \end{pmatrix} \end{array}, \qquad \det{}_{4\times 4} \sim 0, \tag{3·17}$$

$$m_{22} \sim \text{(radiatively induced)}. \tag{3·18}$$

Note that in these textures the 3rd generation is almost decoupled from the other ones. Contrastingly, these textures are of the same form as those of cases 2 and 3 ((3·11) and (3·13)) which are used for the 2nd, 4th and $\bar{4}$th generations to obtain non-zero m_{22}. Therefore, these small eigenvalues m_{22} are strongly affected by the existence of the 4th and $\bar{4}$th generations.

- case 2, 3

We found that there is essentially no candidate in these cases.
One might think that the texture

$$\begin{array}{c} \\ 2 \\ 3 \\ 4 \\ \bar{4} \end{array} \begin{array}{c} \begin{array}{cccc} 2 & 3 & 4 & \bar{4} \end{array} \\ \begin{pmatrix} 0 & 0 & m & 0 \\ 0 & 0 & m & 0 \\ m & m & m & M \\ 0 & 0 & M & \end{pmatrix} \end{array}, \qquad \det{}_{4\times 4} \sim 0, \tag{3·19}$$

reproduces a non-zero eigenvalue m_{22} radiatively. However, in this texture the second and third generations have the same structure. Therefore this matrix has at most rank 3 and yields an almost zero eigenvalue for m_{22} even when all the radiatively induced Yukawa couplings are included. There are two more candidates for texture having hierarchical mass structure:

$$\begin{array}{c} \\ 2 \\ 3 \\ 4 \\ \bar{4} \end{array} \begin{array}{c} \begin{array}{cccc} 2 & 3 & 4 & \bar{4} \end{array} \\ \begin{pmatrix} m & 0 & & 0 \\ 0 & 0 & m & 0 \\ & m & & M \\ 0 & 0 & M & \bar{m} \end{pmatrix} \end{array}, \qquad \det{}_{4\times 4} \sim m^3\bar{m}, \tag{3·20}$$

$$\begin{array}{c} \\ 2 \\ 3 \\ 4 \\ \bar{4} \end{array} \begin{array}{c} \begin{array}{cccc} 2 & 3 & 4 & \bar{4} \end{array} \\ \begin{pmatrix} m & 0 & & 0 \\ 0 & 0 & m & 0 \\ & m & m & M \\ 0 & 0 & M & 0 \end{pmatrix} \end{array}, \qquad \det{}_{4\times 4} \sim 0. \tag{3·21}$$

However, (3·20) and (3·21) coincide with (3·15) and (3·17) by changing the label of the generation ($2 \leftrightarrow 3$). We do not consider these types of texture.*)

In conclusion, we have two candidates, (3·15) and (3·17), which may reproduce hierarchical mass structure between the second and third generations of the up and down sectors.

In addition to the difference between the mass eigenvalues for types A and B, another remarkable difference exists between these two types of texture. As we have already mentioned, it is the infrared behavior of Yukawa couplings that is characteristic to this ANF model. As long as we restrict ourselves to the third generation, two

*) Strictly speaking, we cannot exchange the generation label ($2 \leftrightarrow 3$) when we use one of the textures (3·15) and (3·17) for the up-quark sector and one of (3·20) and (3·21) for the down-quark, and vice versa, for example. This case yields a large mixing angle between generations, which is experimentally excluded.

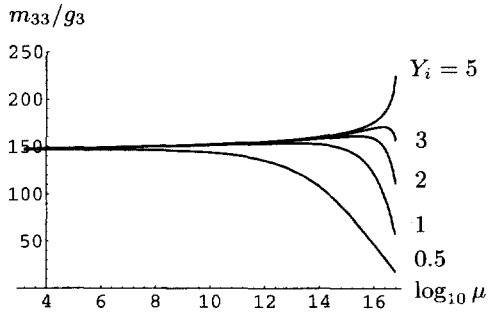

Fig. 1. Typical behavior of m_{33} in the type A texture.

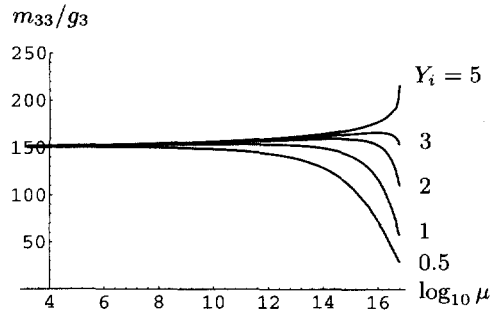

Fig. 2. Typical behavior of m_{33} in the type B texture.

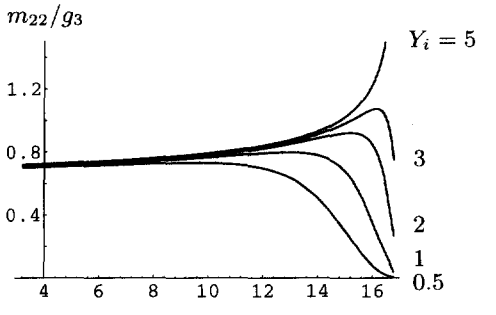

Fig. 3. Typical behavior of m_{22} in the type A texture.

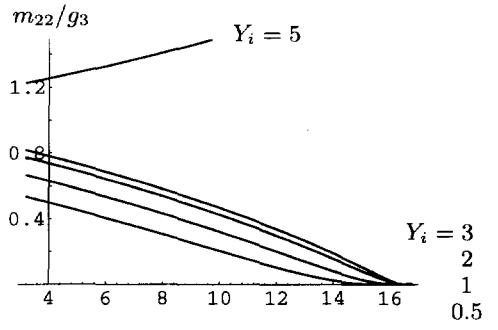

Fig. 4. Typical behavior of m_{22} in the type B texture.

(In the above figures, we set $M_{\rm GUT} = 7 \times 10^{16}$ GeV, $\alpha_{\rm GUT} = 1.0$, $M = 1$ TeV, $\tan\beta = 5$, and all the non-zero Yukawa couplings at $M_{\rm GUT}$ are taken to have the same value Y_i.)

textures have the same infrared structures (Figs. 1 and 2): the Yukawa couplings Y_{33} sit almost on their infrared fixed points at low energy in both cases. However, the infrared behavior of the eigenvalues of the second generation is quite different. For the type A texture, the resultant eigenvalue m_{22} (see (3·16)) is obtained from the tree-level Yukawa couplings (and VEVs whose orders are assumed), and therefore it can be regarded as an infrared fixed point value (Fig. 3). On the other hand, for the type B texture, the eigenvalue m_{22} is induced radiatively by the renormalization procedure and does not reach its theoretical infrared fixed point value at low energy (Fig. 4).

3.2. *Texture for mass matrix*

Next, we discuss which texture can be used for the quark and lepton sectors. From the above discussions we have learned that the type A texture provides us with a mechanism in which we can make full use of infrared fixed points. We see from Fig. 5 that the typical value of the hierarchical factor $\frac{m\bar{m}}{M^2}$ (see (3·16)) is generally $1/100$ or less, and that this factor becomes smaller for larger $\tan\beta$. It is far smaller than the observed strange to bottom mass ratio ($\sim 1/30$). Therefore we do not use

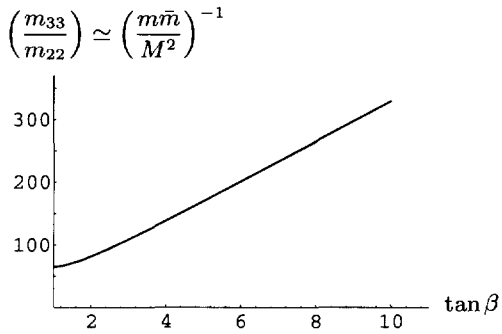

Fig. 5. Typical behavior of the hierarchical factor in the type A texture ($\alpha_{\rm GUT} = 1$, $M = 1$ TeV).

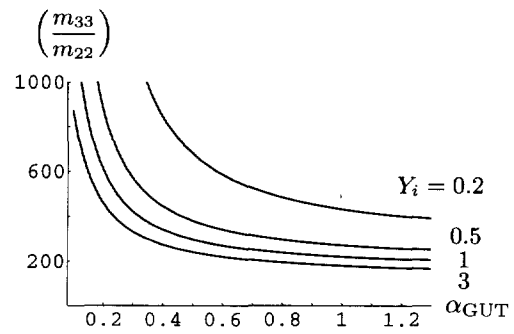

Fig. 6. Typical behavior of the hierarchical factor in the type B texture ($\tan\beta = 5$, $M = 1$ TeV).

the type A texture but adopt the type B one for the down-quark and charged lepton sectors. On the other hand, the hierarchical factor in the up-quark sector, charm to top mass ratio ($\sim 1/250$), is much smaller than the ratio of bottom and strange. We can adopt the type A mass texture for the up-quark sector. Note that in the type A texture, the masses of heavy quarks (charm as well as top) are given by the infrared fixed point values for Yukawa couplings, which are almost insensitive to their initial values at $M_{\rm GUT}$.

Once we fix the texture for the up and down/lepton sectors, we can estimate the quark and lepton masses at low-energy scale. However, there arise two difficulties in reproducing hierarchical structures both in up and down sectors. First, the top and bottom Yukawa couplings reach their infrared fixed point values, which requires a large $\tan\beta$ scenario. This large $\tan\beta$ scenario makes the hierarchical factor in the up sector much smaller than the actual value of the ratio of top and charm (see Fig. 5). Second, the ratio of the eigenvalues, m_{33}/m_{22}, at low energy is found to be at least 100 in the type B texture (Fig. 6).

Some improvement must be made to overcome the above mismatches. It is found that we can remove both difficulties by introducing only one parameter, ϵ, and attaching it to bottom/tau Yukawa couplings. Even when ϵ is introduced, the type A texture cannot be used for the down/lepton sectors, because their non-zero $Y_{\bar{4}\bar{4}}$ elements contribute to the beta-function of the top Yukawa coupling and make its infrared fixed point value far smaller than the experimental one. Then, we finally find that the following mass texture for quark and lepton at the GUT scale can reproduce the low-energy experimental values of the fermion masses:

$$m_U = \begin{array}{c} \\ 2 \\ 3 \\ 4 \\ \bar{4} \end{array} \begin{array}{c} \begin{array}{cccc} 2 & 3 & 4 & \bar{4} \end{array} \\ \begin{pmatrix} 0 & 0 & m & 0 \\ 0 & m & & 0 \\ m & & & M \\ 0 & 0 & M & \bar{m} \end{pmatrix} \end{array}, \tag{3·22}$$

$$m_D = \begin{array}{c} \\ 2 \\ 3 \\ 4 \\ \bar{4} \end{array} \begin{array}{c} \begin{array}{cccc} 2 & 3 & 4 & \bar{4} \end{array} \\ \begin{pmatrix} 0 & 0 & m & 0 \\ 0 & \epsilon m & 0 & 0 \\ m & 0 & m & M \\ 0 & 0 & M & 0 \end{pmatrix} \end{array}, \tag{3·23}$$

$$m_E = \begin{array}{c} \\ 2 \\ 3 \\ 4 \\ \bar{4} \end{array} \begin{array}{c} \begin{array}{cccc} 2 & 3 & 4 & \bar{4} \end{array} \\ \begin{pmatrix} 0 & 0 & 3m & 0 \\ 0 & 3\epsilon m & 0 & 0 \\ 3m & 0 & 3m & M \\ 0 & 0 & M & 0 \end{pmatrix} \end{array}. \tag{3·24}$$

Here we have used the Higgs field of the $\overline{126}$ ($\overline{45}$) representation of $SO(10)$ ($SU(5)$) so that the boundary conditions in the down/lepton sector may correctly reproduce the observed bottom/tau (and strange/mu) ratio, as noted in the previous section. In this texture, all the quark Yukawa couplings except for $\boldsymbol{Y}_{d_{33}}$ converge to their infrared fixed points independently of their initial values at the GUT scale. Within this approximation, this texture leads to the low-energy prediction of fermion masses:*)

$$\begin{aligned} m_t &\sim 180 \text{ GeV}, & m_c &\sim 1.0 \text{ GeV}, \\ m_b &\sim 3.1 \text{ GeV}, & m_s &\sim 0.081 \text{ GeV}, \\ m_\tau &\sim 1.75 \text{ GeV}, & m_\mu &\sim 0.103 \text{ GeV}, \quad (\text{at } M_Z) \end{aligned} \tag{3·25}$$

for the input values

$$\begin{aligned} M_{\text{GUT}} &\sim 5.3 \times 10^{16} \text{ GeV}, & \alpha_{\text{GUT}} &\sim 0.3, & \epsilon &\sim 0.2, \\ M_{\text{SUSY}} &\sim 1 \text{ TeV}, & \tan\beta &\sim 20, & V &\sim 3 \text{ TeV}. \end{aligned} \tag{3·26}$$

These results are surely in good agreement with the present experimental values. For the above input values, both M_{GUT} and α_{GUT} are larger than those of the usual MSSM because of the asymptotically non-free character of this ESSM. It is also noted that ϵ is on the order of the Cabibbo angle. This fact may be naturally reproduced with the anomalous $U(1)$ symmetry,[16] which may be helpful in considering hierarchies between the first and other generations.

3.3. *CKM mixing angles*

Encouraged by the successful predictions of the texture in the previous section, we finally consider full mass matrices including quark mixing angles. This may be done by introducing hierarchically very small Yukawa couplings. As for these very small couplings, we cannot apply the IRFP approach to texture forms in a similar way to the previous section. However, by considering the extension of the above uniquely obtained texture, we can almost fix the Yukawa interactions between all five generations phenomenologically.

As noted in §2, the 1-3 quark mixing is described well by the 1-3 mixing in the up sector and the 1-2 quark mixing by the 1-2 mixing in the down sector. Therefore

*) For simplicity, we set the blanks in m_U (3·22) to be zeros.

the eigenvalue m_{11} for up- (down-) quark sector can be automatically reproduced by introducing a small mixing $\boldsymbol{Y}_{u_{13}}$ ($\boldsymbol{Y}_{d_{12}}$) into our texture. A problem arises in the 2-3 quark mixing for which the usual seesaw-type relation between mixing angle and eigenvalues is not successful. Fortunately, however, in our extended model, the mass eigenvalues for the second generation can be properly reproduced by mixing with the extra vector-like generations. Therefore the 2-3 mixing parameter can be treated independently of the 2-2 mass eigenvalue as long as it does not affect m_{22} very strongly. We can thus adopt the following 3×3 matrices for the ordinary generations in which the CKM mixing angles may be correctly reproduced.

$$(m_U)_{3\times 3} = \begin{array}{c} \\ 1 \\ 2 \\ 3 \end{array} \begin{array}{c} \begin{array}{ccc} 1 & 2 & 3 \end{array} \\ \begin{pmatrix} & & \epsilon^l \\ & & \\ \epsilon^l & & 1 \end{pmatrix} \end{array} \cdot m_t\,, \tag{3·27}$$

$$(m_D)_{3\times 3} = \begin{array}{c} \\ 1 \\ 2 \\ 3 \end{array} \begin{array}{c} \begin{array}{ccc} 1 & 2 & 3 \end{array} \\ \begin{pmatrix} & \epsilon^m & \\ \epsilon^m & & \epsilon^n \\ & \epsilon^n & 1 \end{pmatrix} \end{array} \cdot m_b\,. \tag{3·28}$$

The down-quark (and charged lepton) sector is just the Fritzsch type of texture,[21] in which the mass of the second generation induced by the seesaw mechanism is much smaller than "tree-level" one (see (2·6)), which now comes from mixing with the extra generations. At this point, note that ϵ in the texture in the previous section happens to have just the same value as the Cabibbo mixing angle for explaining all hierarchies in the second and third generations of quarks and leptons. Therefore it is not necessary to introduce any small mixing parameter other than ϵ.

m	$\lvert V_{us}\rvert$
2	0.6
3	0.27
4	0.06

n	$\lvert V_{cb}\rvert$
1	0.17
2	0.035
3	0.007

l	$\lvert V_{ub}\rvert$	m_u
3	0.008	~ 32 MeV
4	0.002	~ 1.3 MeV
5	0.0003	~ 0.5 MeV

(3·29)

m	n	$\lvert V_{ub}\rvert$	m	n	$\lvert V_{ub}\rvert$	m	n	$\lvert V_{ub}\rvert$
2	1	0.044	3	1	0.01	4	1	0.002
2	2	0.009	3	2	0.002	4	2	0.0004
2	3	0.002	3	3	0.0004	4	3	0.0001

(3·30)

After all, there is a reasonable 5×5 GUT-scale texture which explains the experimental values of the CKM mixing angles, and we can see that this texture is actually almost the only possibility left in this situation.

$$m_U \simeq \begin{array}{c} \\ 1 \\ 2 \\ 3 \\ 4 \\ \bar{4} \end{array} \begin{array}{c} \begin{array}{ccccc} 1 & 2 & 3 & 4 & \bar{4} \end{array} \\ \begin{pmatrix} 0 & 0 & \epsilon^4 m & 0 & 0 \\ 0 & 0 & 0 & m & 0 \\ \epsilon^4 m & 0 & m & 0 & 0 \\ 0 & m & 0 & 0 & M \\ 0 & 0 & 0 & M & \bar{m} \end{pmatrix} \end{array}, \tag{3·31}$$

$$m_D \simeq \begin{array}{c} \\ 1 \\ 2 \\ 3 \\ 4 \\ \bar{4} \end{array} \begin{array}{c} \begin{array}{ccccc} 1 & 2 & 3 & 4 & \bar{4} \end{array} \\ \begin{pmatrix} 0 & \epsilon^4 m & 0 & 0 & 0 \\ \epsilon^4 m & 0 & \epsilon^3 m & m & 0 \\ 0 & \epsilon^3 m & \epsilon m & 0 & 0 \\ 0 & m & 0 & m & M \\ 0 & 0 & 0 & M & 0 \end{pmatrix} \end{array}, \tag{3·32}$$

$$m_E \simeq \begin{array}{c} \\ 1 \\ 2 \\ 3 \\ 4 \\ \bar{4} \end{array} \begin{array}{c} \begin{array}{ccccc} 1 & 2 & 3 & 4 & \bar{4} \end{array} \\ \begin{pmatrix} 0 & 3\epsilon^4 m & 0 & 0 & 0 \\ 3\epsilon^4 m & 0 & 3\epsilon^3 m & 3m & 0 \\ 0 & 3\epsilon^3 m & 3\epsilon m & 0 & 0 \\ 0 & 3m & 0 & 3m & M \\ 0 & 0 & 0 & M & 0 \end{pmatrix} \end{array}. \tag{3·33}$$

This texture reproduces the low-energy predictions at M_Z scale:

$$\begin{array}{lll} m_u \sim 2.9 \text{ MeV}, & m_d \sim 4.3 \text{ MeV}, & m_e \sim 0.6 \text{ MeV}, \\ m_c \sim 1.0 \text{ GeV}, & m_s \sim 0.089 \text{ GeV}, & m_\mu \sim 0.104 \text{ GeV}, \\ m_t \sim 180 \text{ GeV}, & m_b \sim 3.1 \text{ GeV}, & m_\tau \sim 1.75 \text{ GeV}, \end{array} \tag{3·34}$$

$$|V_{\text{CKM}}| \simeq \begin{pmatrix} 0.974 & 0.228 & 0.0037 \\ 0.228 & 0.973 & 0.039 \\ 0.005 & 0.039 & 0.999 \end{pmatrix}. \tag{3·35}$$

These values are also nearly consistent with the experimental ones.*)

§4. Summary and discussion

We have investigated the fermion mass matrix structure at the GUT scale in an asymptotically non-free model with a pair of extra generations. The characteristic feature of this model is that the couplings converge to their infrared fixed points very quickly. By making full use of the IR behavior of the couplings, we determined the fermion mass matrices at the GUT scale almost uniquely. We have found the following: i) We can understand the charm quark mass as well as the top in terms of their infrared fixed point values. It is interesting that the hierarchical factor of the top and charm ratio comes from the existence of the 4th and $\bar{4}$th generations at the TeV scale. Also we should like to note that the Yukawa couplings of $Y_{24}(Y_{42})$ reach

*) This V_{CKM} is extracted from the original (unitary) 5×5 CKM matrix, and the other matrix elements are suppressed by large M. The unitarity of V_{CKM} is realized up to 10^{-4} for $M \sim O$ (TeV).

their infrared fixed points with considerable strength. This indicates that the second generation is strongly coupled with the extra generations. ii) Though the masses of the other lighter quarks are not related to the infrared structure for the ANF character, we can determine their mass texture almost uniquely by introducing only one small parameter. It is interesting that this small parameter happens to be equal to the Cabibbo mixing angle. In the down-quark sector the resultant strange-quark mass eigenvalue is suppressed by the existence of the extra generations, as in the up-quark sector, in spite of the appreciable large induced Yukawa coupling Y_{22}. iii) As for the lepton masses, they are reproduced quite successfully by assuming that the relevant Higgs fields belong to $\overline{126}$ representation of $SO(10)$. This is in remarkable contrast to the case of the MSSM in which, as seen from the Georgi-Jarlskog type of texture,[22] one has to assume that the relevant Higgs field must be the mixture of 10 and 126 representations.

In the MSSM case, there are many works containing phenomenological analyses on the fermion mass structure. It is known that, for example, the Fritzsch- and Georgi-Jarlskog-type textures provide us with important hints and standard basis for finding realistic models. Until now, in the ESSM, we have not established a standard texture which reproduces the phenomenological fermion masses well, and the aim of this paper is to establish the form of the possible texture in this model. Then, we would also like to emphasize the importance of the IRFP structure. We think that, particularly in asymptotically non-free theories, the infrared fixed point approach can be one of the attractive selection rule for the texture form, as well as the other methods, e.g. horizontal symmetry. We could surely assign some quantum numbers of $U(1)$ symmetry[16] to each fermion and relevant Higgs particle to reproduce our texture (including ϵ parameter), but our aim here is to establish the possible form of texture first.

It is essential for us to understand the heavier fermion masses as their IR fixed point values that not only the SUSY breaking scale but also the invariant masses of the extra generations are on the order of the TeV scale. This fact implies that when SUSY is discovered, the extra generations may be also found. Using muon colliders[23] in particular, the extra generations may be explored easily, since in our model the second generation couples strongly to the extra generations.

Acknowledgements

We would like to thank T. Kugo and N. Maekawa for many helpful discussions and valuable comments. M. B. is supported in part by the Grant-in Aid for Scientific Research No. 09640375.

Appendix A

—— More Complex Cases ——

In this appendix, we briefly present analyses for two more complex cases. In one case, more than two generations couple to the $\bar{4}$th generation via invariant mass terms and in the other case the form of the texture is non-symmetric.

A.1. *More than two M*

Let us make the classification of hierarchical textures, following the analysis in §3. First, we consider 3×3 texture. In addition to the three cases discussed in §3 ((3·9), (3·11), (3·13)), there are two types of texture which provide a non-zero eigenvalue m_{33}:

- case 4

$$\begin{array}{c} \\ 3 \\ 4 \\ \bar{4} \end{array} \begin{array}{c} \begin{array}{ccc} 3 & 4 & \bar{4} \end{array} \\ \begin{pmatrix} 0 & m & M' \\ m & 0 & M \\ M' & M & 0 \end{pmatrix} \end{array}, \qquad \det{}_{3\times 3} \sim MM'm, \tag{A·1}$$

$$m_{33} \sim \left(\frac{M'}{M}\right) m, \tag{A·2}$$

- case 5

$$\begin{array}{c} \\ 3 \\ 4 \\ \bar{4} \end{array} \begin{array}{c} \begin{array}{ccc} 3 & 4 & \bar{4} \end{array} \\ \begin{pmatrix} 0 & 0 & M' \\ 0 & m & M \\ M' & M & \end{pmatrix} \end{array}, \qquad \det{}_{3\times 3} \sim M'^2 m, \tag{A·3}$$

$$m_{33} \sim \left(\frac{M'}{M}\right)^2 m. \tag{A·4}$$

From the above two textures, we get three types of texture which produce the hierarchical mass eigenvalues $m_{22} \ll m_{33} \ll M, M'$ at low energy without a small parameter ϵ, in addition to the type A and B textures obtained in §3.

- case 4
  - type C

$$\begin{array}{c} \\ 2 \\ 3 \\ 4 \\ \bar{4} \end{array} \begin{array}{c} \begin{array}{cccc} 2 & 3 & 4 & \bar{4} \end{array} \\ \begin{pmatrix} 0 & m & m & M' \\ m & & m & 0 \\ m & m & & M \\ M' & 0 & M & \end{pmatrix} \end{array}, \tag{A·5}$$

- case 5
  - type D

$$\begin{array}{c} \\ 2 \\ 3 \\ 4 \\ \bar{4} \end{array} \begin{array}{c} \begin{array}{cccc} 2 & 3 & 4 & \bar{4} \end{array} \\ \begin{pmatrix} 0 & m & 0 & M' \\ m & m & 0 & 0 \\ 0 & 0 & m & M \\ M' & 0 & M & \end{pmatrix} \end{array}, \tag{A·6}$$

○ type E

$$\begin{array}{c} \\ 2 \\ 3 \\ 4 \\ \bar{4} \end{array} \begin{array}{c} \begin{array}{cccc} 2 & 3 & 4 & \bar{4} \end{array} \\ \begin{pmatrix} & m & & M' \\ m & 0 & m & 0 \\ & m & m & M \\ M' & 0 & M & \end{pmatrix} \end{array} . \tag{A·7}$$

Next we consider a realistic mass texture for quarks and leptons. One can easily see that all the above types of textures have hierarchical factors of order 1/100 or less and no IRFP structure for the 2nd generation, unlike the type A texture. Therefore we must also introduce a (small) parameter ϵ to obtain the hierarchy in the down-quark and/or lepton sector. On the other hand, we can get the hierarchy in the up-quark sector from any one of five textures (type A – E). As mentioned in §3, we adopt the type A texture for the up-quark sector by making active use of the infrared fixed-point structure which is a characteristic feature of this ANF model. Note that due to the $SO(10)$ GUT-like relations for Yukawa couplings to a singlet Higgs, if we adopt the textures of type C – E for the down and lepton sectors we have to add M' to the up-quark texture (the type A texture). These quantities M' change the determinant and thus spoil the hierarchical structure of the type A texture. Therefore we also must include the small parameter ϵ in the invariant mass term M'. Taking into account all issues discussed to this point, we searched the realistic textures of quark and lepton at the GUT scale and found no candidate to reproduce the present experimental data of hierarchical mass eigenvalues, except for the one obtained in §3.

A.2. *Non-symmetric texture*

Until this point, we have implicitly taken the textures to be of symmetric forms. Another more general analysis is to consider non-symmetric types of texture. However, the general analysis is too complex and is not particularly physically meaningful. Therefore we suppose the up-type texture to be of the type A. We made numerical analyses of the types of 4×4 texture for the down-quark and charged lepton sectors which reproduce the hierarchical mass ratios charm/top, strange/bottom, mu/tau, etc., without the small parameter ϵ. Even in this situation, we found no realistic candidate, except for the one obtained in §3.

Appendix B

—— The Renormalization-Group Equations ——

We present the 2-loop beta-functions for gauge couplings of $SU(3)_C \times SU(2)_W \times U(1)_Y$ and the 1-loop beta-functions for Yukawa couplings. Here we neglect the CP phase, which does not affect the numerical results. The evolution of gauge coupling constants is given by

$$\frac{dg_i}{dt} = b_i \frac{g_i^3}{16\pi^2} + \frac{g_i^3}{(16\pi^2)^2} \left[\sum_j b_{ij} g_j^2 - \sum_{a=u,d,e} c_{ia} \left(\mathrm{Tr}(\boldsymbol{Y}_a^T \boldsymbol{Y}_a) + Y_{\bar{a}}^2 \right) \right.$$

$$-\sum_{k=1}^{4}\sum_{X=Q,u,d,L,e} d_{iX}Y_{X_k}^2\Bigg], \tag{B·1}$$

where $b_i = (10.6, 5, 1)$ for $U(1)_Y$ (in a GUT normalization), $SU(2)_W$ and $SU(3)_C$ respectively, and

$$b_{ij} = \begin{pmatrix} 977/75 & 39/5 & 88/3 \\ 13/5 & 53 & 40 \\ 11/3 & 15 & 178/3 \end{pmatrix}, \tag{B·2}$$

$$c_{ia} = \begin{matrix} u & d & e \end{matrix} \\ \begin{pmatrix} 26/5 & 14/5 & 18/5 \\ 6 & 6 & 2 \\ 4 & 4 & 0 \end{pmatrix}, \tag{B·3}$$

$$d_{iX} = \begin{matrix} Q & u & d & L & e \end{matrix} \\ \begin{pmatrix} 2/5 & 16/5 & 4/5 & 6/5 & 12/5 \\ 6 & 0 & 0 & 2 & 0 \\ 4 & 2 & 2 & 0 & 0 \end{pmatrix}. \tag{B·4}$$

The beta-functions for Yukawa couplings in the superpotential (3·4) are given as follows:

$$\frac{d\boldsymbol{Y}_{a\,ij}}{dt} = \frac{1}{16\pi^2}\beta_{a_{ij}}, \quad (a = u, d, e) \tag{B·5}$$

$$\frac{dY_{\tilde{a}}}{dt} = \frac{1}{16\pi^2}\beta_{\tilde{a}}, \quad (a = u, d, e) \tag{B·6}$$

$$\frac{dY_{X_i}}{dt} = \frac{1}{16\pi^2}\beta_{X_i}, \quad (X = Q, u, d, L, e) \tag{B·7}$$

$$\frac{dY}{dt} = \frac{1}{16\pi^2}\beta_Y, \tag{B·8}$$

$$\beta_{u_{ij}} = \boldsymbol{Y}_{u\,ij}\left[3\mathrm{Tr}(\boldsymbol{Y}_u^T\boldsymbol{Y}_u) + 3Y_{\tilde{d}}^2 + Y_{\tilde{e}}^2 - \frac{16}{3}g_3^2 - 3g_2^2 - \frac{13}{15}g_1^2\right] + \left(3\boldsymbol{Y}_u\boldsymbol{Y}_u^T\boldsymbol{Y}_u + \boldsymbol{Y}_u\boldsymbol{Y}_d^T\boldsymbol{Y}_d\right)_{ij} + \sum_k\left(\boldsymbol{Y}_{u\,kj}Y_{Q_i}Y_{Q_k} + \boldsymbol{Y}_{u\,ik}Y_{u_k}Y_{u_j}\right), \tag{B·9}$$

$$\beta_{d_{ij}} = \boldsymbol{Y}_{d\,ij}\left[\mathrm{Tr}(3\boldsymbol{Y}_d^T\boldsymbol{Y}_d + \boldsymbol{Y}_e^T\boldsymbol{Y}_e) + 3Y_{\tilde{u}}^2 - \frac{16}{3}g_3^2 - 3g_2^2 - \frac{7}{15}g_1^2\right] + \left(3\boldsymbol{Y}_d\boldsymbol{Y}_d^T\boldsymbol{Y}_d + \boldsymbol{Y}_d\boldsymbol{Y}_u^T\boldsymbol{Y}_u\right)_{ij} + \sum_k\left(\boldsymbol{Y}_{d\,kj}Y_{Q_i}Y_{Q_k} + \boldsymbol{Y}_{d\,ik}Y_{d_k}Y_{d_j}\right), \tag{B·10}$$

$$\beta_{e_{ij}} = \boldsymbol{Y}_{e\,ij}\left[\mathrm{Tr}(3\boldsymbol{Y}_d^T\boldsymbol{Y}_d + \boldsymbol{Y}_e^T\boldsymbol{Y}_e) + 3Y_{\tilde{u}}^2 - 3g_2^2 - \frac{9}{5}g_1^2\right] + 3\left(\boldsymbol{Y}_e\boldsymbol{Y}_e^T\boldsymbol{Y}_e\right)_{ij} + \sum_k\left(\boldsymbol{Y}_{e\,kj}Y_{L_i}Y_{L_k} + \boldsymbol{Y}_{e\,ik}Y_{e_k}Y_{e_j}\right), \tag{B·11}$$

$$\beta_{\tilde{u}} = Y_{\tilde{u}}\Bigg[\mathrm{Tr}(3\boldsymbol{Y}_d^T\boldsymbol{Y}_d + \boldsymbol{Y}_e^T\boldsymbol{Y}_e) + 6Y_{\tilde{u}}^2 + Y_{\tilde{d}}^2 + \sum_i\left(Y_{Q_i}^2 + Y_{u_i}^2\right)$$

$$-\frac{16}{3}g_3^2 - 3g_2^2 - \frac{13}{15}g_1^2\Bigg], \tag{B·12}$$

$$\beta_{\bar{d}} = Y_{\bar{d}}\Bigg[\mathrm{Tr}(3\boldsymbol{Y}_u^T\boldsymbol{Y}_u) + Y_{\bar{u}}^2 + 6Y_{\bar{d}}^2 + Y_{\bar{e}}^2 + \sum_i \left(Y_{Q_i}^2 + Y_{d_i}^2\right)$$
$$-\frac{16}{3}g_3^2 - 3g_2^2 - \frac{7}{15}g_1^2\Bigg], \tag{B·13}$$

$$\beta_{\bar{e}} = Y_{\bar{e}}\left[\mathrm{Tr}(3\boldsymbol{Y}_u^T\boldsymbol{Y}_u) + 3Y_{\bar{d}}^2 + 4Y_{\bar{e}}^2 + \sum_i \left(Y_{L_i}^2 + Y_{e_i}^2\right) - 3g_2^2 - \frac{9}{5}g_1^2\right], \tag{B·14}$$

$$\beta_{Q_i} = Y_{Q_i}\Bigg[Y_{\bar{u}}^2 + Y_{\bar{d}}^2 + \sum_j \left(8Y_{Q_j}^2 + 3Y_{u_j}^2 + 3Y_{d_j}^2 + 2Y_{L_j}^2 + Y_{e_j}^2\right) + Y^2$$
$$-\frac{16}{3}g_3^2 - 3g_2^2 - \frac{1}{15}g_1^2\Bigg] + \sum_k Y_{Q_k}\left(\boldsymbol{Y}_u^T\boldsymbol{Y}_u + \boldsymbol{Y}_d^T\boldsymbol{Y}_d\right)_{ik}, \tag{B·15}$$

$$\beta_{u_i} = Y_{u_i}\Bigg[2Y_{\bar{u}}^2 + \sum_j \left(6Y_{Q_j}^2 + 5Y_{u_j}^2 + 3Y_{d_j}^2 + 2Y_{L_j}^2 + Y_{e_j}^2\right) + Y^2$$
$$-\frac{16}{3}g_3^2 - \frac{16}{15}g_1^2\Bigg] + \sum_k 2Y_{u_k}\left(\boldsymbol{Y}_u^T\boldsymbol{Y}_u\right)_{ik}, \tag{B·16}$$

$$\beta_{d_i} = Y_{d_i}\Bigg[2Y_{\bar{d}}^2 + \sum_j \left(6Y_{Q_j}^2 + 3Y_{u_j}^2 + 5Y_{d_j}^2 + 2Y_{L_j}^2 + Y_{e_j}^2\right) + Y^2$$
$$-\frac{16}{3}g_3^2 - \frac{4}{15}g_1^2\Bigg] + \sum_k 2Y_{d_k}\left(\boldsymbol{Y}_d^T\boldsymbol{Y}_d\right)_{ik}, \tag{B·17}$$

$$\beta_{L_i} = Y_{L_i}\Bigg[Y_{\bar{e}}^2 + \sum_j \left(6Y_{Q_j}^2 + 3Y_{u_j}^2 + 3Y_{d_j}^2 + 4Y_{L_j}^2 + Y_{e_j}^2\right) + Y^2$$
$$-3g_2^2 - \frac{3}{5}g_1^2\Bigg] + \sum_k Y_{L_k}\left(\boldsymbol{Y}_e^T\boldsymbol{Y}_e\right)_{ik}, \tag{B·18}$$

$$\beta_{e_i} = Y_{e_i}\Bigg[2Y_{\bar{e}}^2 + \sum_j \left(6Y_{Q_j}^2 + 3Y_{u_j}^2 + 3Y_{d_j}^2 + 2Y_{L_j}^2 + 3Y_{e_j}^2\right) + Y^2$$
$$-\frac{12}{5}g_1^2\Bigg] + \sum_k 2Y_{e_k}\left(\boldsymbol{Y}_e^T\boldsymbol{Y}_e\right)_{ik}, \tag{B·19}$$

$$\beta_Y = 3Y\left[\sum_i \left(6Y_{Q_i}^2 + 3Y_{u_i}^2 + 3Y_{d_i}^2 + 2Y_{L_i}^2 + Y_{e_i}^2\right) + Y^2\right]. \tag{B·20}$$

References

1) C. Giunti, C. W. Kim and U. W. Lee, Mod. Phys. Lett. **A6** (1991), 1745.
J. Ellis, S. Kelley and D. V. Nanopoulos, Phys. Lett. **260B** (1991), 131.
U. Amaldi, W. de Boer and H. Fürstenau, Phys. Lett. **260B** (1991), 447.
P. Langacker and M. Luo, Phys. Rev. **D44** (1991), 817.
2) S. Raby, hep-ph/9501349.

Z. Berezhiani, hep-ph/9602325, and references therein.
H. Arason, D. J. Castano, E. J. Piard and P. Ramond, Phys. Rev. **D47** (1992), 232.
V. Barger, M. S. Berger and P. Ohmann, Phys. Rev. **D47** (1992), 1093.
3) P. Langacker and N. Polonsky, Phys. Rev. **D49** (1994), 1454; **D50** (1994), 2199.
N. Polonsky, Phys. Rev. **D54** (1996), 4537.
4) M. Bando, J. Sato, T. Onogi and T. Takeuchi, Phys. Rev. **D56** (1997), 1589.
5) M. Bando, J. Sato and K. Yoshioka, Prog. Theor. Phys. **98** (1997), 169.
6) M. Bando, hep-ph/9705237, and references therein.
7) I. Antoniadis, J. Ellis, S. Kelley and D. V. Nanopoulos, Phys. Lett. **272B** (1991), 31.
D. Bailin and A. Love, Phys. Lett. **280B** (1992), 26; Mod. Phys. Lett. **A7** (1992), 1485.
A. E. Faraggi, Phys. Lett. **302B** (1993), 202.
8) J. C. Pati, Phys. Lett. **228B** (1989), 228.
K. S. Babu, J. C. Pati and H. Stremnitzer, Phys. Lett. **256B** (1991), 206; **264B** (1991), 347; Phys. Rev. Lett. **67** (1991), 1688; Phys. Rev. **D51** (1995), 2451.
K. S. Babu, J. C. Pati and X. Zhang, Phys. Rev. **D46** (1992), 2190.
K. S. Babu and J. C. Pati, Phys. Rev. **D48** (1993), 1921.
9) L. Maiani, G. Parisi and R. Petronzio, Nucl. Phys. **B136** (1978), 115.
S. Kelley, J. L. Lopez and D. V. Nanopoulos, Phys. Lett. **274B** (1992), 387.
B. Brahmachari, U. Sarkar and K. Sridhar, Mod. Phys. Lett. **A8** (1993), 3349.
S. P. Martin and P. Ramond, Phys. Rev. **D51** (1995), 6515.
K. S. Babu and J. C. Pati, Phys. Lett. **384B** (1996), 140.
D. Ghilencea, M. Lanzagorta and G. G. Ross, Nucl. Phys. **B511** (1998), 3; Phys. Lett. **415B** (1997), 253.
10) M. E. Peskin and T. Takeuchi, Phys. Rev. Lett. **65** (1990), 964; Phys. Rev. **D46** (1992), 381.
L. Lavoura and J. P. Silva, Phys. Rev. **D47** (1993), 2046.
N. Maekawa, Prog. Theor. Phys. **93** (1995), 919.
11) T. Moroi, H. Murayama and T. Yanagida, Phys. Rev. **D48** (1993), 2995.
K. Fujikawa, Prog. Theor. Phys. **92** (1994), 1149.
12) M. Lanzagorta and G. G. Ross, Phys. Lett. **349B** (1995), 319.
B. C. Allanach and S. F. King, Nucl. Phys. **B473** (1996), 3; **B507** (1997), 91.
13) G. G. Ross, Phys. Lett. **364B** (1995), 216.
14) P. Ramond, R. G. Roberts and G. G. Ross, Nucl. Phys. **B406** (1993), 19.
15) M. Leurer, Y. Nir and N. Seiberg, Nucl. Phys. **B398** (1993), 319; **B420** (1994), 468.
P. Pouliot and N. Seiberg, Phys. Lett. **318B** (1993), 169.
16) L. Ibáñez and G. G. Ross, Phys. Lett. **332B** (1994), 100.
P. Binétruy and P. Ramond, Phys. Lett. **350B** (1995), 49.
E. Dudas, S. Pokorski and C. A. Savoy, Phys. Lett. **356B** (1995), 45.
P. Binétruy, S. Lavignac and P. Ramond, Nucl. Phys. **B477** (1996), 353.
T. Kobayashi and H. Nakano, Nucl. Phys. **B496** (1997), 103.
17) H. Fusaoka and Y. Koide, Phys. Rev. **D57** (1998), 3986.
18) Particle Data Group, Phys. Rev. **D54** (1996), 1.
19) R. Gatto, G. Sartori and M. Tonin, Phys. Lett. **28B** (1968), 128.
R. J. Oakes, Phys. Lett. **29B** (1969), 683.
H. Fritzsch, Nucl. Phys. **B155** (1979), 189.
20) D. Ng and Y. J. Ng, Mod. Phys. Lett. **A6** (1991), 2243.
G. F. Giudice, Mod. Phys. Lett. **A7** (1992), 2429.
W.-S. Hou and G.-G. Wong, Phys. Rev. **D52** (1995), 5269.
21) H. Fritzsch, Phys. Lett. **73B** (1978), 317; Nucl. Phys. **B155** (1979), 189.
H. Georgi and D. V. Nanopoulos, Nucl. Phys. **B155** (1979), 52.
22) H. Georgi and C. Jarlskog, Phys. Lett. **86B** (1979), 297.
J. A. Harvey, P. Ramond and D. B. Reiss, Phys. Lett. **92B** (1980), 309.
S. Dimopoulos, L. J. Hall and S. Raby, Phys. Rev. Lett. **68** (1992), 1984.
23) For recent reviews,
J. F. Gunion, talk given at the Fermilab Workshop on Physics at the First Muon Collider and at the Front End of a Muon Collider, November 1997, hep-ph/9802258.
V. Barger, talk given at the 4th International Conference on the Physics Potential and Development of $\mu^+\mu^-$ Colliders, San Francisco, December 1997, hep-ph/9803480.